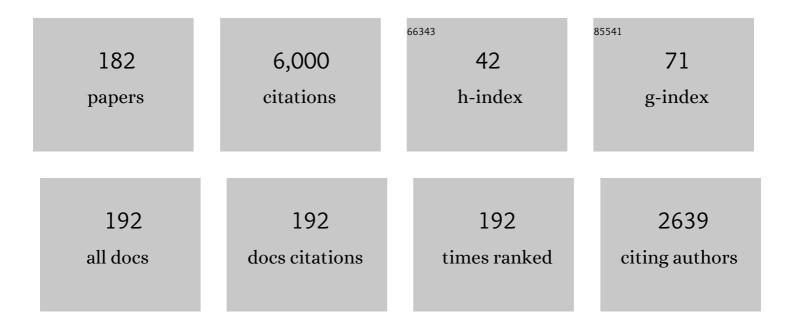
List of Publications by Year in descending order

Source: https://exaly.com/author-pdf/5303867/publications.pdf Version: 2024-02-01



KAZUSHI ASAMUDA

#	Article	IF	CITATIONS
1	The Space Physics Environment Data Analysis System (SPEDAS). Space Science Reviews, 2019, 215, 9.	8.1	332
2	The Analyzer of Space Plasmas and Energetic Atoms (ASPERA-3) for the Mars Express Mission. Space Science Reviews, 2007, 126, 113-164.	8.1	241
3	The Analyser of Space Plasmas and Energetic Atoms (ASPERA-4) for the Venus Express mission. Planetary and Space Science, 2007, 55, 1772-1792.	1.7	214
4	Solar Wind-Induced Atmospheric Erosion at Mars: First Results from ASPERA-3 on Mars Express. Science, 2004, 305, 1933-1936.	12.6	204
5	Geospace exploration project ERG. Earth, Planets and Space, 2018, 70, .	2.5	201
6	Solar wind proton reflection at the lunar surface: Low energy ion measurement by MAPâ€₽ACE onboard SELENE (KAGUYA). Geophysical Research Letters, 2008, 35, .	4.0	178
7	The loss of ions from Venus through the plasma wake. Nature, 2007, 450, 650-653.	27.8	168
8	Extremely high reflection of solar wind protons as neutral hydrogen atoms from regolith in space. Planetary and Space Science, 2009, 57, 2132-2134.	1.7	130
9	The ERG Science Center. Earth, Planets and Space, 2018, 70, .	2.5	124
10	In-flight Performance and Initial Results of Plasma Energy Angle and Composition Experiment (PACE) onÂSELENE (Kaguya). Space Science Reviews, 2010, 154, 265-303.	8.1	123
11	First observation of a miniâ€magnetosphere above a lunar magnetic anomaly using energetic neutral atoms. Geophysical Research Letters, 2010, 37, .	4.0	114
12	Plasma Acceleration Above Martian Magnetic Anomalies. Science, 2006, 311, 980-983.	12.6	111
13	Carbon dioxide photoelectron energy peaks at Mars. Icarus, 2006, 182, 371-382.	2.5	105
14	Mass composition of the escaping plasma at Mars. Icarus, 2006, 182, 320-328.	2.5	103
15	Mars Express and Venus Express multi-point observations of geoeffective solar flare events in December 2006. Planetary and Space Science, 2008, 56, 873-880.	1.7	102
16	Simultaneous appearance of isolated auroral arcs and Pc 1 geomagnetic pulsations at subauroral latitudes. Journal of Geophysical Research, 2008, 113, .	3.3	91
17	Time of flight analysis of pulsating aurora electrons, considering waveâ€particle interactions with propagating whistler mode waves. Journal of Geophysical Research, 2010, 115, .	3.3	91
18	Medium energy neutral atom (MENA) imager for the IMAGE mission. Space Science Reviews, 2000, 91, 113-154.	8.1	90

#	Article	IF	CITATIONS
19	Structure of the martian wake. Icarus, 2006, 182, 329-336.	2.5	81
20	First direct detection of ions originating from the Moon by MAPâ€PACE IMA onboard SELENE (KAGUYA). Geophysical Research Letters, 2009, 36, .	4.0	79
21	Solarâ€wind proton access deep into the nearâ€Moon wake. Geophysical Research Letters, 2009, 36, .	4.0	79
22	Relation between fine structure of energy spectra for pulsating aurora electrons and frequency spectra of whistler mode chorus waves. Journal of Geophysical Research: Space Physics, 2015, 120, 7728-7736.	2.4	73
23	Relativistic Electron Microbursts as Highâ€Energy Tail of Pulsating Aurora Electrons. Geophysical Research Letters, 2020, 47, e2020GL090360.	4.0	66
24	Location of the bow shock and ion composition boundaries at Venus—initial determinations from Venus Express ASPERA-4. Planetary and Space Science, 2008, 56, 780-784.	1.7	64
25	First in situ observation of the Moonâ€originating ions in the Earth's Magnetosphere by MAPâ€PACE on SELENE (KAGUYA). Geophysical Research Letters, 2009, 36, .	4.0	62
26	First medium energy neutral atom (MENA) Images of Earth's magnetosphere during substorm and storm-time. Geophysical Research Letters, 2001, 28, 1147-1150.	4.0	61
27	Medium-energy particle experiments—electron analyzer (MEP-e) for the exploration of energization and radiation in geospace (ERG) mission. Earth, Planets and Space, 2018, 70, .	2.5	57
28	Numerical interpretation of high-altitude photoelectron observations. Icarus, 2006, 182, 383-395.	2.5	56
29	Remote energetic neutral atom imaging of electric potential over a lunar magnetic anomaly. Geophysical Research Letters, 2013, 40, 262-266.	4.0	56
30	Electric fields within the martian magnetosphere and ion extraction: ASPERA-3 observations. Icarus, 2006, 182, 337-342.	2.5	54
31	Electron oscillations in the induced martian magnetosphere. Icarus, 2006, 182, 360-370.	2.5	54
32	First ENA observations at Mars: ENA emissions from the martian upper atmosphere. Icarus, 2006, 182, 424-430.	2.5	53
33	Low-energy charged particle measurement by MAP-PACE onboard SELENE. Earth, Planets and Space, 2008, 60, 375-385.	2.5	53
34	Empirical energy spectra of neutralized solar wind protons from the lunar regolith. Journal of Geophysical Research, 2012, 117, .	3.3	53
35	Pairwise energy gainâ€loss feature of solar wind protons in the nearâ€Moon wake. Geophysical Research Letters, 2009, 36, .	4.0	51
36	Ionospheric plasma acceleration at Mars: ASPERA-3 results. Icarus, 2006, 182, 308-319.	2.5	48

#	Article	IF	CITATIONS
37	Comparative analysis of Venus and Mars magnetotails. Planetary and Space Science, 2008, 56, 812-817.	1.7	48
38	Energetic neutral atom imaging of the lunar surface. Journal of Geophysical Research: Space Physics, 2013, 118, 3937-3945.	2.4	47
39	Medium-energy particle experiments–ion mass analyzer (MEP-i) onboard ERG (Arase). Earth, Planets and Space, 2017, 69, .	2.5	47
40	Scientific objectives and instrumentation of Mercury Plasma Particle Experiment (MPPE) onboard MMO. Planetary and Space Science, 2010, 58, 182-200.	1.7	45
41	Energetic neutral atom observations of magnetic anomalies on the lunar surface. Journal of Geophysical Research, 2012, 117, .	3.3	44
42	The source region and its characteristic of pulsating aurora based on the Reimei observations. Journal of Geophysical Research, 2011, 116, .	3.3	43
43	Low-energy particle experiments–electron analyzer (LEPe) onboard the Arase spacecraft. Earth, Planets and Space, 2017, 69, .	2.5	43
44	First ENA observations at Mars: Subsolar ENA jet. Icarus, 2006, 182, 413-423.	2.5	42
45	Protons in the nearâ€lunar wake observed by the Subâ€keV Atom Reflection Analyzer on board Chandrayaanâ€1. Journal of Geophysical Research, 2010, 115, .	3.3	42
46	Auroral particle instrument onboard the index satellite. Advances in Space Research, 2003, 32, 375-378.	2.6	41
47	Sheared flows and smallâ€scale Alfvén wave generation in the auroral acceleration region. Geophysical Research Letters, 2009, 36, .	4.0	41
48	Biogenic oxygen from Earth transported to the Moon by a wind of magnetospheric ions. Nature Astronomy, 2017, 1, .	10.1	40
49	First ENA observations at Mars: Charge exchange ENAs produced in the magnetosheath. Icarus, 2006, 182, 431-438.	2.5	39
50	Low-energy particle experiments–ion mass analyzer (LEPi) onboard the ERG (Arase) satellite. Earth, Planets and Space, 2018, 70, .	2.5	39
51	PFISR and ROPA observations of pulsating aurora. Journal of Atmospheric and Solar-Terrestrial Physics, 2009, 71, 708-716.	1.6	37
52	A new view on the solar wind interaction with the Moon. Geoscience Letters, 2015, 2, .	3.3	37
53	Observations of magnetic anomaly signatures in Mars Express ASPERA-3 ELS data. Icarus, 2006, 182, 396-405.	2.5	36
54	Low energy neutral atom imaging on the Moon with the SARA instrument aboard Chandrayaan-1 mission. Journal of Earth System Science, 2005, 114, 749-760.	1.3	35

#	Article	IF	CITATIONS
55	Plasma intrusion above Mars crustal fields—Mars Express ASPERA-3 observations. Icarus, 2006, 182, 406-412.	2.5	35
56	lon escape at Mars: Comparison of a 3-D hybrid simulation with Mars Express IMA/ASPERA-3 measurements. Icarus, 2006, 182, 350-359.	2.5	34
57	Development of the multi-spectral auroral camera onboard the index satellite. Advances in Space Research, 2003, 32, 379-384.	2.6	33
58	The Energization and Radiation in Geospace (ERG) Project. Geophysical Monograph Series, 0, , 103-116.	0.1	33
59	Pre-flight Calibration and Near-Earth Commissioning Results of the Mercury Plasma Particle Experiment (MPPE) Onboard MMO (Mio). Space Science Reviews, 2021, 217, 1.	8.1	32
60	Development of an ion energy mass spectrometer for application on board three-axis stabilized spacecraft. Review of Scientific Instruments, 2005, 76, 014501.	1.3	31
61	Scattering function for energetic neutral hydrogen atoms off the lunar surface. Geophysical Research Letters, 2011, 38, n/a-n/a.	4.0	30
62	Small and mesoâ€scale properties of a substorm onset auroral arc. Journal of Geophysical Research, 2010, 115, .	3.3	29
63	Cross-scale coupling in the auroral acceleration region. Geophysical Research Letters, 2011, 38, n/a-n/a.	4.0	29
64	First direct observation of sputtered lunar oxygen. Journal of Geophysical Research: Space Physics, 2014, 119, 709-722.	2.4	29
65	Auroral Plasma Acceleration Above Martian Magnetic Anomalies. Space Science Reviews, 2007, 126, 333-354.	8.1	28
66	First ENA observations at Mars: Solar-wind ENAs on the nightside. Icarus, 2006, 182, 439-447.	2.5	27
67	Significance of Wave-Particle Interaction Analyzer for direct measurements of nonlinear wave-particle interactions. Annales Geophysicae, 2013, 31, 503-512.	1.6	25
68	Rocket observation of energetic electrons in the low-altitude auroral ionosphere during the DELTA campaign. Earth, Planets and Space, 2006, 58, 1155-1163.	2.5	24
69	Development of an LENA instrument for planetary missions by numerical simulations. Planetary and Space Science, 2007, 55, 1518-1529.	1.7	24
70	Coordinated EISCAT Svalbard radar and Reimei satellite observations of ion upflows and suprathermal ions. Journal of Geophysical Research, 2008, 113, .	3.3	24
71	Identification of substorm onset location and preonset sequence using Reimei, THEMIS GBO, PFISR, and Geotail. Journal of Geophysical Research, 2010, 115, .	3.3	24
72	Motion of aurorae. Geophysical Research Letters, 2010, 37, .	4.0	23

#	Article	IF	CITATIONS
73	Energetic Neutral Atoms (ENA) at Mars: Properties of the hydrogen atoms produced upstream of the martian bow shock and implications for ENA sounding technique around non-magnetized planets. Icarus, 2006, 182, 448-463.	2.5	22
74	The Venusian induced magnetosphere: A case study of plasma and magnetic field measurements on the Venus Express mission. Planetary and Space Science, 2008, 56, 796-801.	1.7	22
75	Backscattered energetic neutral atoms from the Moon in the Earth's plasma sheet observed by Chandarayaanâ€1/Subâ€keV Atom Reflecting Analyzer instrument. Journal of Geophysical Research: Space Physics, 2014, 119, 3573-3584.	2.4	22
76	Solar wind plasma protrusion into the martian magnetosphere: ASPERA-3 observations. Icarus, 2006, 182, 343-349.	2.5	21
77	IMF Direction Derived from Cycloid-Like Ion Distributions Observed by Mars Express. Space Science Reviews, 2007, 126, 239-266.	8.1	21
78	Software-type Wave–Particle Interaction Analyzer on board the Arase satellite. Earth, Planets and Space, 2018, 70, .	2.5	21
79	First observation of energetic neutral atoms in the Venus environment. Planetary and Space Science, 2008, 56, 807-811.	1.7	19
80	Small satellite REIMEI for auroral observations. Acta Astronautica, 2011, 69, 499-513.	3.2	19
81	Lowâ€energy ion precipitation structures associated with pulsating auroral patches. Journal of Geophysical Research: Space Physics, 2015, 120, 5408-5431.	2.4	19
82	Cusp type electrostatic analyzer for measurements of medium energy charged particles. Review of Scientific Instruments, 2006, 77, 123303.	1.3	18
83	Spatial charge cloud size of microchannel plates. Review of Scientific Instruments, 2007, 78, 023302.	1.3	18
84	ENA detection in the dayside of Mars: ASPERA-3 NPD statistical study. Planetary and Space Science, 2008, 56, 840-845.	1.7	18
85	Ground-based observations of diffuse auroral structures in conjunction with Reimei measurements. Annales Geophysicae, 2010, 28, 873-881.	1.6	18
86	Ion hole formation and nonlinear generation of electromagnetic ion cyclotron waves: THEMIS observations. Geophysical Research Letters, 2017, 44, 8730-8738.	4.0	18
87	ERG – A small-satellite mission to investigate the dynamics of the inner magnetosphere. Advances in Space Research, 2006, 38, 1861-1869.	2.6	17
88	Geospace exploration project: Arase (ERG). Journal of Physics: Conference Series, 2017, 869, 012095.	0.4	17
89	Structure of the ionized lunar sodium and potassium exosphere: Dawnâ€dusk asymmetry. Journal of Geophysical Research E: Planets, 2014, 119, 798-809.	3.6	16
90	Medium Energy Neutral Atom (MENA) Imager for the Image Mission. , 2000, , 113-154.		16

#	Article	IF	CITATIONS
91	High-resolution detection of 100keV electrons using avalanche photodiodes. Nuclear Instruments and Methods in Physics Research, Section A: Accelerators, Spectrometers, Detectors and Associated Equipment, 2008, 594, 50-55.	1.6	15
92	Imaging the South Pole–Aitken basin in backscattered neutral hydrogen atoms. Planetary and Space Science, 2015, 115, 57-63.	1.7	15
93	Simultaneous Pulsating Aurora and Microburst Observations With Groundâ€Based Fast Auroral Imagers and CubeSat FIREBIRDâ€II. Geophysical Research Letters, 2021, 48, e2021GL094494.	4.0	14
94	In situ observations of ions and magnetic field around Phobos: the mass spectrum analyzer (MSA) for the Martian Moons eXploration (MMX) mission. Earth, Planets and Space, 2021, 73, .	2.5	14
95	Interaction between terrestrial plasma sheet electrons and the lunar surface: SELENE (Kaguya) observations. Geophysical Research Letters, 2010, 37, .	4.0	13
96	Fine scale structures of pulsating auroras in the early recovery phase of substorm using groundâ€based EMCCD camera. Journal of Geophysical Research, 2012, 117, .	3.3	13
97	Highâ€speed MCP anodes for high time resolution lowâ€energy charged particle spectrometers. Journal of Geophysical Research: Space Physics, 2017, 122, 1816-1830.	2.4	13
98	Instantaneous Frequency Analysis on Nonlinear EMIC Emissions: Arase Observation. Geophysical Research Letters, 2018, 45, 13,199.	4.0	13
99	Evening Side EMIC Waves and Related Proton Precipitation Induced by a Substorm. Journal of Geophysical Research: Space Physics, 2021, 126, e2020JA029091.	2.4	13
100	Avalanche photodiode for measurement of low-energy electrons. Nuclear Instruments and Methods in Physics Research, Section A: Accelerators, Spectrometers, Detectors and Associated Equipment, 2005, 545, 744-752.	1.6	12
101	High time resolution measurement of multiple electron precipitations with energy-time dispersion in high-latitude part of the cusp region. Journal of Geophysical Research, 2005, 110, .	3.3	12
102	Scattering characteristics and imaging of energetic neutral atoms from the Moon in the terrestrial magnetosheath. Journal of Geophysical Research: Space Physics, 2016, 121, 432-445.	2.4	12
103	Data processing in Software-type Wave–Particle Interaction Analyzer onboard the Arase satellite. Earth, Planets and Space, 2018, 70, .	2.5	12
104	The Effect of Depletion Layer Thickness in Avalanche Photodiodes for Measurement of Low-energy Electrons. Nuclear Instruments and Methods in Physics Research, Section A: Accelerators, Spectrometers, Detectors and Associated Equipment, 2006, 566, 575-583.	1.6	11
105	Reimei observation of highly structured auroras caused by nonaccelerated electrons. Journal of Geophysical Research, 2010, 115, .	3.3	11
106	Spatial-temporal characteristics of flickering aurora as seen by high-speed EMCCD imaging observations. Journal of Geophysical Research, 2011, 116, n/a-n/a.	3.3	11
107	Cross-Energy Couplings from Magnetosonic Waves to Electromagnetic Ion Cyclotron Waves through Cold Ion Heating inside the Plasmasphere. Physical Review Letters, 2021, 127, 245101.	7.8	11
108	Density Depletions Associated With Enhancements of Electron Cyclotron Harmonic Emissions: An ERG Observation. Geophysical Research Letters, 2018, 45, 10,075.	4.0	10

#	Article	IF	CITATIONS
109	Cusp and Nightside Auroral Sources of O ⁺ in the Plasma Sheet. Journal of Geophysical Research: Space Physics, 2019, 124, 10036-10047.	2.4	10
110	KAGUYA observation of global emissions of indigenous carbon ions from the Moon. Science Advances, 2020, 6, eaba1050.	10.3	10
111	Investigation of Small cale Electron Density Irregularities Observed by the Arase and Van Allen Probes Satellites Inside and Outside the Plasmasphere. Journal of Geophysical Research: Space Physics, 2021, 126, e2020JA027917.	2.4	10
112	Discovery of proton hill in the phase space during interactions between ions and electromagnetic ion cyclotron waves. Scientific Reports, 2021, 11, 13480.	3.3	10
113	Collaborative Research Activities of the Arase and Van Allen Probes. Space Science Reviews, 2022, 218, .	8.1	10
114	Venusian bow shock as seen by the ASPERAâ€4 ion instrument on Venus Express. Journal of Geophysical Research, 2010, 115, .	3.3	9
115	Nongyrotropic electron velocity distribution functions near the lunar surface. Journal of Geophysical Research, 2012, 117, .	3.3	9
116	Transport of solar wind plasma onto the lunar nightside surface. Geophysical Research Letters, 2016, 43, 10,586.	4.0	9
117	Exploration of energization and radiation in geospace (ERG): challenges, development, and operation of satellite systems. Earth, Planets and Space, 2018, 70, .	2.5	9
118	Substormâ€Associated Ionospheric Flow Fluctuations During the 27 March 2017 Magnetic Storm: SuperDARNâ€Arase Conjunction. Geophysical Research Letters, 2018, 45, 9441-9449.	4.0	9
119	Design of a mission network system using SpaceWire for scientific payloads onboard the Arase spacecraft. Earth, Planets and Space, 2018, 70, .	2.5	9
120	Mission Data Processor Aboard the BepiColombo Mio Spacecraft: Design and Scientific Operation Concept. Space Science Reviews, 2020, 216, 1.	8.1	9
121	Plasmoid formation for multiple onset substorms: observations of the Japanese Lunar Mission "Kaguya". Annales Geophysicae, 2009, 27, 59-64.	1.6	8
122	A noise attenuation method for medium-energy electron measurements in the radiation belt. Advances in Space Research, 2009, 43, 792-801.	2.6	8
123	Spatial evolution of frictional heating and the predicted thermospheric wind effects in the vicinity of an auroral arc measured with the Sondrestrom incoherentâ€scatter radar and the Reimei satellite. Journal of Geophysical Research, 2009, 114, .	3.3	8
124	Fine-scale dynamics of black auroras obtained from simultaneous imaging and particle observations with the Reimei satellite. Journal of Geophysical Research, 2011, 116, n/a-n/a.	3.3	8
125	Long Term Operability of Li-ion Battery under Micro-gravity Condition Demonstrated by the Satellite "REIMEI". Electrochemistry, 2016, 84, 12-16.	1.4	8
126	Statistical Properties of Molecular Ions in the Ring Current Observed by the Arase (ERG) Satellite. Geophysical Research Letters, 2019, 46, 8643-8651.	4.0	8

#	Article	IF	CITATIONS
127	Energetic neutral atom imaging mass spectroscopy of the Moon and Mercury environments. Advances in Space Research, 2006, 37, 38-44.	2.6	7
128	Application of single-sided silicon strip detector to energy and charge state measurements of medium energy ions in space. Nuclear Instruments and Methods in Physics Research, Section A: Accelerators, Spectrometers, Detectors and Associated Equipment, 2009, 603, 355-360.	1.6	7
129	Smallâ€scale magnetic fields on the lunar surface inferred from plasma sheet electrons. Geophysical Research Letters, 2013, 40, 3362-3366.	4.0	7
130	Electron properties in invertedâ€V structures and their vicinities based on Reimei observations. Journal of Geophysical Research: Space Physics, 2014, 119, 3650-3663.	2.4	7
131	Solar wind scattering from the surface of Mercury: Lessons from the Moon. Icarus, 2017, 296, 39-48.	2.5	7
132	Electron Energy Spectrum and Auroral Power Estimation From Incoherent Scatter Radar Measurements. Journal of Geophysical Research: Space Physics, 2018, 123, 6865-6887.	2.4	7
133	Arase Observation of the Source Region of Auroral Arcs and Diffuse Auroras in the Inner Magnetosphere. Journal of Geophysical Research: Space Physics, 2020, 125, e2019JA027310.	2.4	7
134	Multiâ€Event Analysis of Plasma and Field Variations in Source of Stable Auroral Red (SAR) Arcs in Inner Magnetosphere During Nonâ€Stormâ€Time Substorms. Journal of Geophysical Research: Space Physics, 2021, 126, e2020JA029081.	2.4	7
135	Multipoint Measurement of Fineâ€Structured EMIC Waves by Arase, Van Allen Probe A and Ground Stations. Geophysical Research Letters, 2021, 48, e2021GL096488.	4.0	7
136	Simultaneous observation of the electron acceleration and ion deceleration in the dayside high-latitude auroral region. Geophysical Research Letters, 2003, 30, .	4.0	6
137	Development of an APD With Large Area and Thick Depletion Layer for Energetic Electron Measurements in Space. IEEE Transactions on Nuclear Science, 2010, 57, 1549-1555.	2.0	6
138	Estimating high-energy electron fluxes by intercalibrating Reimei optical and particle measurements using an ionospheric model. Journal of Atmospheric and Solar-Terrestrial Physics, 2012, 89, 8-17.	1.6	6
139	Kaguya observation of the ion acceleration around a lunar crustal magnetic anomaly. Planetary and Space Science, 2014, 93-94, 87-95.	1.7	6
140	Filtering-Based Three-Axis Attitude Determination Package for Spinning Spacecraft: Preliminary Results with Arase. Aerospace, 2020, 7, 97.	2.2	6
141	Active auroral arc powered by accelerated electrons from very high altitudes. Scientific Reports, 2021, 11, 1610.	3.3	6
142	Fieldâ€Aligned Lowâ€Energy O ⁺ Flux Enhancements in the Inner Magnetosphere Observed by Arase. Journal of Geophysical Research: Space Physics, 2021, 126, e2021JA029168.	2.4	6
143	An Overview and Initial In-Orbit Status of INDEX S , 2005, , .		6
144	First measurement of â^1⁄410 keV neutral atoms in the low-latitude ionosphere. Geophysical Research Letters, 1999, 26, 33-36.	4.0	5

#	Article	IF	CITATIONS
145	Medium Energy Ion Mass Spectrometer Capable of Measurements of Three-Dimensional Distribution Functions in Space. IEEE Transactions on Plasma Science, 2008, 36, 841-847.	1.3	4
146	Spatial characteristics of wave-like structures in diffuse aurora obtained using optical observations. Annales Geophysicae, 2012, 30, 1693-1701.	1.6	4
147	INTERACTION OF SOLAR WIND WITH MOON: AN OVERVIEW ON THE RESULTS FROM THE SARA EXPERIMENT ABOARD CHANDRAYAAN-1. , 2012, , 35-55.		4
148	Contribution of Electron Pressure to Ring Current and Ground Magnetic Depression Using RAM‧CB Simulations and Arase Observations During 7–8 November 2017 Magnetic Storm. Journal of Geophysical Research: Space Physics, 2021, 126, e2021JA029109.	2.4	4
149	Study of an equatorward detachment of auroral arc from the oval using groundâ€space observations and the BATSâ€Râ€US – CIMI model. Journal of Geophysical Research: Space Physics, 2021, 126, e2020JA029080.	2.4	4
150	Numerical modeling of electron energy-time dispersions in the high-latitude part of the cusp region. Journal of Geophysical Research, 2005, 110, .	3.3	3
151	A LENA Instrument onboard BepiColombo and Chandrayaan-1. , 2009, , .		3
152	The Link Between Wedge‣ike and Nose‣ike Ion Spectral Structures in the Inner Magnetosphere. Geophysical Research Letters, 2021, 48, e2021GL093930.	4.0	3
153	First Simultaneous Observation of a Night Time Mediumâ€Scale Traveling Ionospheric Disturbance From the Ground and a Magnetospheric Satellite. Journal of Geophysical Research: Space Physics, 2021, 126, e2020JA029086.	2.4	3
154	LOW ENERGY CHARGED PARTICLE MEASUREMENT BY JAPANESE LUNAR ORBITER SELENE. , 0, , 33-43.		3
155	Optical and particle observations of type B red aurora. Geophysical Research Letters, 2009, 36, .	4.0	2
156	Fine-Scale Characteristics of Black Aurora and its Generation Process. Geophysical Monograph Series, 0, , 271-278.	0.1	2
157	Energyâ€Resolved Detection of Precipitating Electrons of 30–100ÂkeV by a Sounding Rocket Associated With Dayside Chorus Waves. Journal of Geophysical Research: Space Physics, 2021, 126, e2020JA028477.	2.4	2
158	Lowâ€Altitude Ion Upflow Observed by EISCAT and its Effects on Supply of Molecular Ions in the Ring Current Detected by Arase (ERG). Journal of Geophysical Research: Space Physics, 2021, 126, e2020JA028951.	2.4	2
159	Arase Observation of Simultaneous Electron Scatterings by Upperâ€Band and Lowerâ€Band Chorus Emissions. Geophysical Research Letters, 2021, 48, e2021GL093708.	4.0	2
160	Rocket Observation of Subâ€Relativistic Electrons in the Quiet Dayside Auroral Ionosphere. Journal of Geophysical Research: Space Physics, 2021, 126, e2020JA028633.	2.4	2
161	Magnetic Field and Energetic Particle Flux Oscillations and Highâ€Frequency Waves Deep in the Inner Magnetosphere During Substorm Dipolarization: ERG Observations. Journal of Geophysical Research: Space Physics, 2021, 126, e2020JA029095.	2.4	2
162	The Analyzer of Space Plasmas and Energetic Atoms (ASPERA-3) for the Mars Express Mission. , 2007, , 113-164.		2

#	Article	IF	CITATIONS
163	Flux Enhancements of Fieldâ€Aligned Lowâ€Energy O ⁺ Ion (FALEO) in the Inner Magnetosphere: A Possible Source of Warm Plasma Cloak and Oxygen Torus. Journal of Geophysical Research: Space Physics, 2022, 127, .	2.4	2
164	A new type of rocket-borne neutral atom analyzer. Review of Scientific Instruments, 2000, 71, 3024-3030.	1.3	1
165	Microburst cusp ion precipitation observed with Reimei. Journal of Geophysical Research, 2008, 113, .	3.3	1
166	Ion-dispersion and rapid electron fluctuations in the cusp: a case study. Annales Geophysicae, 2008, 26, 2485-2502.	1.6	1
167	Development of a low-energy charged particle detector with on-anode ASIC for in-situ plasma measurement in the Earthâ $\in^{\rm IMS}$ magnetosphere. , 2009, , .		1
168	Evidence for a Multi-scale Aurora. , 2011, , 271-280.		1
169	First negative system of N ₂ ⁺ in aurora: simultaneous space-borne and ground-based measurements and modeling results. Annales Geophysicae. 2014. 32. 499-506.	1.6	1
170	Spin-Axis Tilt Estimation for Spinning Spacecraft. , 2016, , .		1
171	Auroral Plasma Acceleration above Martian Magnetic Anomalies. , 2007, , 333-354.		1
172	In-flight Performance and Initial Results of Plasma Energy Angle and Composition Experiment (PACE) on SELENE (Kaguya). , 2010, , 265-303.		1
173	Statistical Survey of Arase Satellite Data Sets in Conjunction With the Finnish Riometer Network. Journal of Geophysical Research: Space Physics, 2022, 127, .	2.4	1
174	Signatures of Auroral Potential Structure Extending Through the Nearâ€Equatorial Inner Magnetosphere. Geophysical Research Letters, 2022, 49, .	4.0	1
175	Collisional interactions of precipitating energetic neutral atoms with upper-atmospheric particles in the low-latitude region. Journal of Geophysical Research, 2000, 105, 15861-15873.	3.3	0
176	Flexible Operation System for the Microsatellite 'REIMEI' (INDEX). , 2006, , .		0
177	Development of a Measurement Technique for Medium-Energy Electrons. , 2009, , .		0
178	Next-Generation Plasma Particle Measurements in the Medium Energy Range: Development of Cusp Type Electrostatic Analyser and Ion Mass Spectrometer. , 2009, , .		0
179	Charge and Discharge Performance of the Lithium-ion Secondary Battery in Space. Transactions of the Japan Society for Aeronautical and Space Sciences Aerospace Technology Japan, 2014, 12, Pf_27-Pf_32.	0.2	0
180	Internal Impedance of the Lithium-Ion Secondary Cells Used for Reimei Satellite after the Eleven Years Operation in Space. E3S Web of Conferences, 2017, 16, 07005.	0.5	0

0

#	Article	IF	CITATIONS
181	Extremely Collimated Electron Beams in the High Latitude Magnetosphere Observed by Arase. Geophysical Research Letters, 2021, 48, e2020GL090522.	4.0	Ο

182 IMF Direction Derived from Cycloid-Like Ion Distributions Observed by Mars Express. , 2007, , 239-266.